ELSEVIER Artificial Intelligence in Medicine 13 (1998) 81–97

Artificial Intelligence in Medicine

Computer models of hippocampal circuit changes of the kindling model of epilepsy

William W. Lytton *, Kevin M. Hellman, Thomas P. Sutula

Departments of Neurology and Anatomy and Center for Neuroscience, University of Wisconsin, Wm. S. Middleton VA Hospital, 1300 University Ave., MSC 1715, Madison, WI 53706, USA

Received 28 February 1997; received in revised form 30 October 1997; accepted 15 December 1997

Abstract

Abnormalities in the organization of brain circuits may underlie many types of epilepsy. This hypothesis can best be evaluated in the case of temporal lobe epilepsy, where evidence of rewiring (synaptic reorganization) can be found in the dentate gyrus. Computer modeling of normal and reorganized dentate gyrus was used to understand the functional consequences of these structural changes. Hyperexcitability appeared to be largely limited by the powerful intrinsic adaptation characteristic of granule cells, the principal cells in this area. Combining disinhibition with new recurrent excitatory circuitry was necessary to produce repeated firing of these cells. Paradoxically, continuing regenerative activity was only seen with a large reduction in the strength of the inciting stimulus. Validation of these findings will require further physiological correlation.

Keywords: Computer simulation; Partial epilepsy; Hippocampus; Dentate gyrus; Kindling; Cortical synchronization

* Corresponding author. Tel: +1 608 2653524; fax: +1 608 2622327; e-mail: billl@neurosim.wisc.edu

0933-3657/98/$19.00
PII S0933-3657(98)00005-0

1. Introduction

While transient alterations in cellular activation dynamics may produce the single seizure seen in the setting of stress, lack of sleep or inadequate nutrition, there is substantial evidence that the repeated seizures characteristic of epilepsy reflect alterations in the patterns of connectivity in neuronal networks of the brain. A variety of hypotheses, some competing and some complementary, seek to explain how rewiring of brain circuits could produce repeated seizures. One concept, extensively studied in models by Traub and coworkers [41–45], is that reduction in inhibitory connection strength can lead to epilepsy. It has been hypothesized that reduction in inhibition might occur not only through direct loss of inhibitory neurons or reduction in inhibitory synaptic strength but also through cell death in the hilus or through reduced excitatory drive onto interneurons (dormant basket cell hypothesis) [5,36]. Similarly, it is believed that circumstances leading to increases in excitatory synapse strength or number of excitatory synapses could also produce epilepsy.

Focal seizures are pathological waves of electrical hypersynchrony that may spread from an initial focus in one part of the brain to involve the entire brain. Temporal lobe epilepsy is a syndrome which results in recurrent seizures emerging from the temporal lobe, a common focus of seizure onset. Analysis of the hippocampus from surgically removed temporal lobes of people with epilepsy demonstrates major anatomical changes in the dentate gyrus, a part of the hippocampus [4,3,15]. These anatomical changes include evidence for cell death and for the formation of new synaptic connections as axons sprout. In recent years, evidence has accumulated to demonstrate how both normal and pathological factors could lead to this sort of reorganization in brain circuits [21,22,24]. Repeated seizures, the hallmark of epilepsy, have been shown to be particularly efficacious in this regard [12,20,47]. However, the physiological implications of these wiring alterations are not well understood.

Although the dentate gyrus has a relatively simple anatomy compared to many other brain areas, the connectivity in this area may still involve as many as 30 anatomically distinct cell types [1]. However, despite the varying morphologies, only three cell types can be clearly identified physiologically by differences in firing characteristics [33,34]. A first approximation to the circuit can therefore be made using the three major cell types that have been both anatomically and physiologically defined (Fig. 1). The principal cell of the dentate gyrus is the granule cell (GC), located in a specific granule cell layer. GCs get input from entorhinal cortex via the perforant path (PP) and project to area CA3 of hippocampus via mossy fibers. The other two cell types that we model, inhibitory aspiny interneurons (AC) and excitatory mossy cells (MC), reside largely in the hilus, although some ACs lie in the GC layer. Of the nine connections possible between the three cell types modeled, six appear to be of particular importance in the normal dentate gyrus. Two are feed forward excitatory projections: GC → AC, GC → MC. Two are feedback inhibitory projections: AC → GC, AC → MC. Two involve sign reversal due to synapsing onto an inhibitory cell: MC → AC, AC → AC.

The PP is the principal input into the structure and can be directly stimulated in vitro. Although there is likely to be some PP projection onto other cell types, it is primarily onto GCs. In the current model the primary PP input was onto GCs. Low strength PP input onto the other cell types was also added in some simulations and did not alter the results shown. The principal output is via mossy fibers that are projections from the GCs. Thus, the principal flow of information is from PP to GC to mossy fiber [18]. The other cell types can be viewed as modifying the signal as it is filtered by the GCs.

Kindling is an experimental procedure whereby repeated brain stimulation induces epilepsy in a rat by first evoking repeated seizures which then lead to the spontaneous seizures characteristic of epilepsy. These functional changes induced by kindling are permanent, suggesting underlying structural alterations. In fact, both the axonal sprouting and cell death seen in human epileptics are also seen in kindled rats, where they can be studied in more detail [14,16,20,28,38,39,47]. The cells that die include MCs and some ACs; GCs are relatively spared [35]. Mossy fiber axons of GCs sprout into areas denervated by the seizure-induced cell loss. Although this mossy fiber sprouting is excitatory and, at least in part, forms synapses with other GCs, the potential exists for recurrent excitation in this cell population. It would seem likely that the structural reorganization induced by neuron loss and mossy fiber sprouting will alter the activity of GCs.

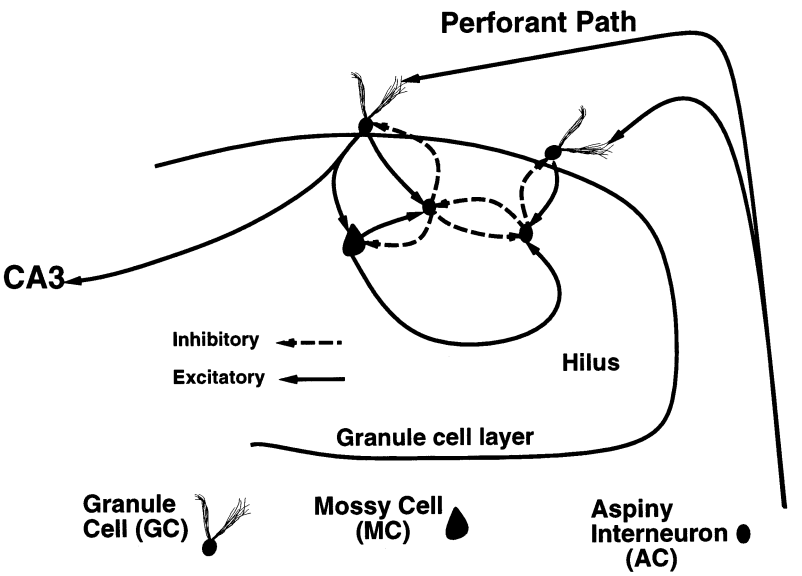

Fig. 1. Circuit diagram showing major features of dentate gyrus connectivity. Other connections present in the model are mentioned in the text but omitted here for clarity. The granule cell layer is represented by the curved line, the hilus is the area that lies within. Cell bodies of the GCs have dendrites that protrude outward where they are contacted by the PP, the major input pathway. The GCs project via mossy fibers to the cells of the hilus (mossy cells and aspiny interneurons). Other branches of the mossy fibers form the main output pathway from dentate gyrus to area CA3 of hippocampus. In MFS, other branches form which make connections between GCs.

The complexity of structural and functional alterations induced by kindling make it difficult to determine straightforward structure/function relationships experimentally. Physiological changes in GC activity after kindling have been surprisingly difficult to demonstrate in in vitro hippocampal slices. The functional consequences of cell death and sprouting remain unclear.

2. Methods

Compartmental models were utilized to recreate the principal cells in the dentate gyrus. GC and MC models had two compartments, while the AC model neuron had one. Simulations were run in NEURON (Hines 1989) [13]. Intrinsic neuron parameters were largely determined by comparison to current-clamp experiments performed in slice. In general, the parameter space necessary to reproduce the electrophysiological responses to depolarization and hyperpolarization at the single cell level model was fairly narrow.

The GC had somatic and dendritic compartments of the same dimensions (length = 200 μ; diameter = 10 μ). Between the compartments, there was 250 Ω cm axial resistance. Channel parameters were taken from Pinsky and Rinzel (1994) [26], with modification of channel densities as required to reproduce the firing patterns of the different cell types. The somatic compartment contained fast sodium and delayed rectifier potassium conductances. The maximum conductance values were $\bar{g}_{Na} = 30$ mS/cm^2 and $\bar{g}_{kdr} = 15$ mS/cm^2, respectively. The dendritic compartment contained an L-type calcium channel ($\bar{g}_{CaL} = 10$ mS/cm^2), a calcium-sensitive potassium channel ($\bar{g}_{AHP} = 10$ mS/cm^2) and a voltage and calcium-sensitive potassium channel ($\bar{g}_{C} = 100$ mS/cm^2). Both the soma and dendrite contained leak conductances: ($\bar{g}_{leak} = 0.1$ mS/cm^2). Capacitance was 2 μF/cm^2. A first-order calcium decay mechanism was present in the dendrite ($\tau = 100$ ms). The input resistance at steady state was 66 MΩ and the membrane time constant was 23 ms. These values were comparable to measurements using impalement [32] and whole cell patch [37].

The MC had a soma, length = 100 μ diameter = 50 μ, with a dendrite length = 200 μ diameter = 10 μ. Axial resistance, membrane capacitance, and membrane resistance were identical to the GC. Except for maximal conductances, channel parameters and locations were the same as in the GC: $\bar{g}_{Na} = 30$ mS/cm^2, $\bar{g}_{kdr} = 20$ mS/cm^2, $\bar{g}_{CaL} = 5$ mS/cm^2, $\bar{g}_{AHP} = 10$ mS/cm^2, $\bar{g}_{C} = 130$ mS/cm^2. The time constant for calcium decay in the dendrite was 1 s. Input resistance at steady state was 120 MΩ with membrane time constant of 24 ms. These values are comparable to previous impalement measurements [6,32].

The AC was a single compartment (length = 100 μ; diameter = 10 μ). This cell contained only two active channels: $\bar{g}_{Na} = 10$ mS/cm^2 and $\bar{g}_{kdr} = 5$ mS/cm^2. Leak conductance was $\bar{g}_{leak} = 0.2$ mS/cm^2. The input resistance at steady state was 154 MΩ to give a membrane time constant of 10 ms. These values were comparable to experiment by Scharfman [32].

$GABA_A$, $GABA_B$, AMPA and NMDA were modeled using a 2-state model [8,17]. Synaptic parameters, except for maximal conductances, were similar to those used in previous studies [9,19]. PP synapses onto GCs were approximated from published voltage clamp [37]. AMPA and NMDA $\bar{g}$ on to GCs were 4.8 and 25 nS, respectively, with a reversal potential of 0 mV. The inhibitory conductance from ACs onto GCs had maximum conductance of 60 nS for $GABA_A$ and 10 nS for $GABA_B$. The other conductances were estimated from published dual cell impalements [34]. The inhibitory conductances from ACs onto MCs were $GABA_A$ $\bar{g}$ of 90 nS and $GABA_B$ $\bar{g}$ 18 nS. Each GC to AC $\bar{g}$ was 2.6 nS AMPA and 6 nS NMDA. Each GC to MC $\bar{g}$ was 1 nS AMPA. Each MC to GC $\bar{g}$ was 1 nS AMPA. Each MC to AC $\bar{g}$ was 3 nS AMPA.

Activity in the network was generally initiated by brief activation of the AMPA and NMDA channels on GCs simulating PP stimulation. Afterwards, ACs provided feedback inhibition and MCs feedback excitation.

The network contained 50 GCs, two ACs, and two MCs. These numbers represent a scaled-down version of the ratio of cells found in the dentate gyrus [2] and are close to the ratio found in a computer generated anatomical model [25]. Detailed connectivity was randomized. Convergence and divergence were initially estimated using data on frequency of connections found doing dual impalements [34]. These values were improved by comparing individual synaptic strengths from dual impalement to population synaptic strengths assessed with voltage clamp of perforant path stimulation. Each GC excited a single random AC and random MC. Every GC was inhibited by two ACs. Each MC excited 25 random GCs and two inhibitory cells. Every MC was inhibited by two inhibitory cells. These connections represented the normal network.

Mossy fiber sprouting was simulated by adding excitatory synaptic conductances. Maximal synaptic conductance due to mossy fiber sprouting was estimated to be comparable to maximal conductance seen with PP stimulation based on current source density recordings in kindled rats [12]. Multiple levels of recurrent connectivity in granule cells were simulated. Although GCs may excite other GCs after kindling and seizures induced by kainic acid [7,40,47], the amount of connectivity remains an important question. We examined the results of stimulation at different percent connectivities to predict the range that would be consistent with physiological results.

3. Results

A variety of parameter sets were assessed in running over 500 simulations with different levels of mossy fiber sprouting (MFS). The response to various levels of MFS reported were robust across parameter variations, although the percentage MFS levels where particular behaviors occurred varied somewhat. Simulations with larger and smaller networks with the same proportions gave similar results, although smaller networks showed more variability between identical simulations with different initial randomization.

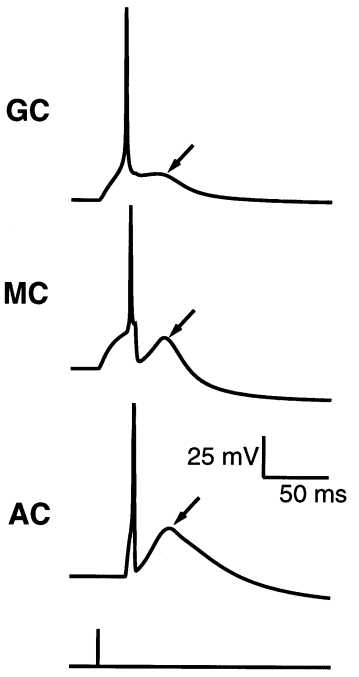

Fig. 2. Single spike firing in all three cell types in response to PP stimulation. Out of the 54 cells in the network, only one voltage trace is shown for each cell type. Other neurons of the same type show very similar firing. In most preparations, inhibitory postsynaptic potentials are negative (hyperpolarizing) but they tend to be depolarizing in dentate gyrus (arrows).

3.1. Normal dentate gyrus produces little firing

GC firing in response to physiological stimulation of perforant path is known to be very restricted, with individual neurons typically firing only a single spike [10]. Using neuron dynamics established from single cell studies and synaptic strengths obtained from dual impalement and voltage-clamp research, this network behavior served as a constraint to determine the connectivity matrix.

In the model, PP excitation produced a single spike after a brief latency in all GCs (Fig. 2). The voltage trace from a single neuron of each cell type is shown, since all of the cells of a type fire in a similar manner, differing only slightly due to initial randomization of individual cell parameters. The GC latency could be shortened with higher conductance of PP synapses. MC spiking followed due both to direct PP input and due to feed-forward excitation from the GCs. The major factor behind the relative delay in MC spiking was the longer time constant for this cell type. Feed-forward excitation from GC and MC to AC resulted in subsequent AC spiking. Feedback inhibition from the ACs was paradoxically seen as a nominally excitatory depolarizing postsynaptic potential (arrows) due to the depolarized position of the γ-amino-butyric acid type-A receptor ($GABA_A$) reversal

potential relative to rest. Although the depolarization associated with this postsynaptic potential would appear to suggest an excitatory effect, paired pulse stimulation demonstrated that the primary effect was in fact inhibitory (Fig. 3). After the first stimulation produced the typical activation sequence, the second, identical, stimulation is completely ineffective in producing another spike in the GC despite the underlying depolarization. The efficacy of inhibition in the setting of depolarization is caused by the increase in conductance associated with synaptic activation. This shunting inhibition effectively short circuits subsequent excitatory conductance changes.

3.2. Effect of disinhibition

Bicuculline is a pharmacological agent that blocks the activation of $GABA_A$, the receptor responsible for this shunting inhibition. Thus, addition of bicuculline could be expected to remove most feedback inhibition from the network. In the dentate gyrus in vitro preparation, bicuculline generally produces little effect on GC firing with single PP stimulation [11]. This is somewhat surprising since bicuculline can produce quite dramatic effects including repetitive firing in other parts of the hippocampus [42].

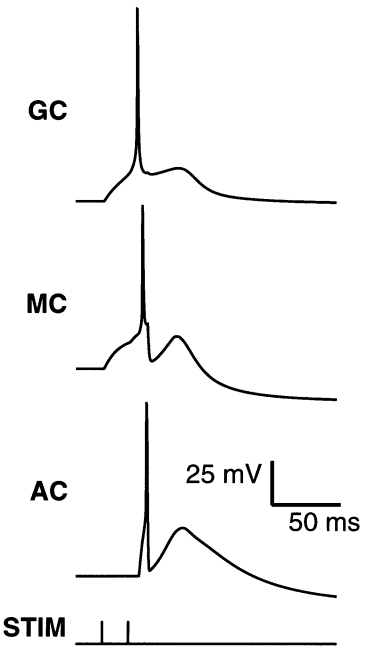

Fig. 3. Paired pulse stimulation. Depolarizing inhibitory potentials are effective in preventing the occurrence of a second spike in response to the second stimulation. One trace is shown for each cell type. Stimulation times are given in the schematic below (stim). Significant delay to cell firing is introduced by the combination of synaptic delay and the intrinsic time constant of the neurons.

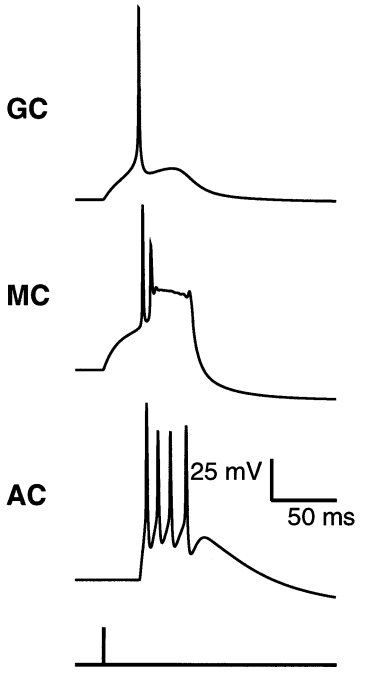

Fig. 4. Disinhibition by blockade of $GABA_A$ inhibitory synapses (bicuculline simulation). One trace is shown for each cell type. GC firing is unchanged from Fig. 2. Mossy cell (MC) shows sustained depolarization leading to depolarization spike blockade. AC shows multiple spike firing.

To simulate the effect of bicuculline in the model, we set $GABA_A$ synaptic strength to 0 without changing any other parameters, eliminating feedback inhibition (Fig. 4). The result was far more spiking in the ACs, released from their own recurrent inhibition. A sustained depolarization was produced in the MCs that was sufficient to inactivate sodium channels in this cell type, producing a depolarization blockade that prevented further spiking. The clear disinhibitory effect on these neurons is further demonstration of the efficacy of shunting inhibition despite the depolarizing postsynaptic potential. Despite these dramatic manifestations of hyperexcitability in the other cell types, the single spike pattern of GC firing was unchanged. This can be explained by noting that GCs have strong intrinsic adaptation that can be demonstrated by noting their very limited spiking under conditions of sustained single-cell current injection [33]. This intrinsic adaptation serves as a form of internal inhibition that restricts firing. Since GC firing is the usual experimentally measured quantity, most experiments would give no indication of the important changes in the activity of the other neurons that the model predicts. In particular, the substantial, sustained depolarization in the MC is a potential cause of the cell death that appears to be a feature of the progression towards epilepsy.

3.3. Mossy fiber sprouting

The targets of MFS from GCs remain uncertain. For these studies, we were primarily interested in assessing the potential of MFS for producing hyperexcitability. Therefore, we made the assumption that all MFS would be onto other GCs (GC → GC), yielding new recurrent excitatory circuit with no new offsetting inhibitory circuitry. We made the strength of GC → GC MFS connections the same as the strength of PP synaptic inputs onto GCs, noting that in vivo studies had demonstrated comparably-sized synaptic current sinks [12].

In Fig. 5 the raster plot at top indicates the activity in all GCs; each point represents a single spike. The voltage trace of a single representative GC is shown at the bottom. All GCs spike at approximately the same time with variation that can be largely explained by initial parameter variation. At low sprouting percentages, the usual single-spike behavior is seen in the GCs. With somewhat higher MFS, multiple spikes are produced, something that is not seen physiologically with inhibition intact. Although our method of estimating mossy fiber sprouting synaptic strength is imprecise, we can predict that the physiological data are consistent with quite low levels ($< 5\%$) of MFS.

Even with much higher sprouting levels, activity always remained brief and self-limiting with no evidence of the continued regenerative activity that might be expected due to the recurrent excitatory connectivity. As in the disinhibited case, the strong GC adaptation appeared to limit firing.

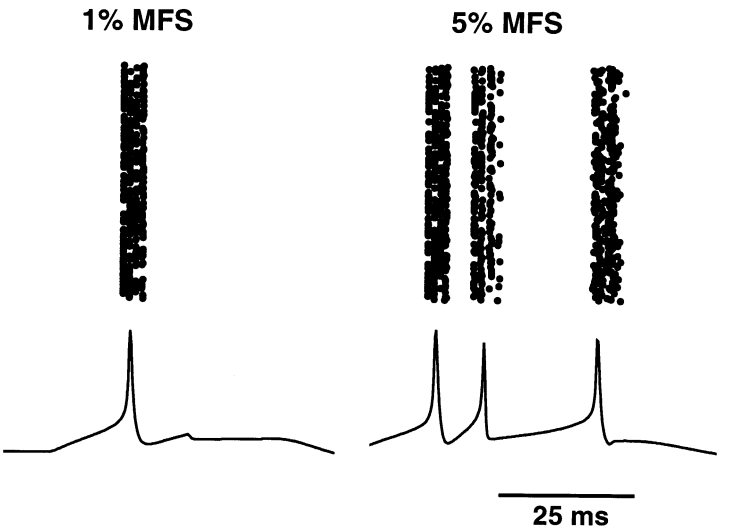

Fig. 5. Firing of GCs in network with 1 and 5% MFS in response to PP stimulation. Representative voltage trace of a single GC is shown at bottom in each case. Raster plots at top show firing times (x-axis) of spikes for all 50 GCs in the network (y-axis). Note that with 1% sprouting each cell fires only once; foreshortening of the y-axis gives a false appearance of multiple spikes.

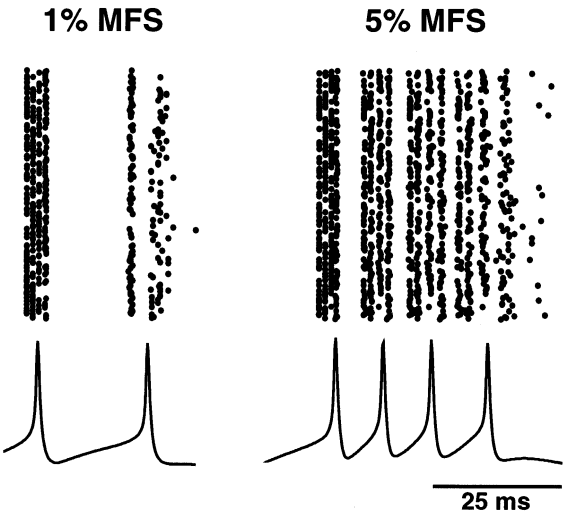

Fig. 6. Firing of GCs in $GABA_A$ disinhibited network (bicuculline simulation) with 1 and 5% MFS in response to PP stimulation. More prolonged bursting is seen at each level of mossy fiber sprouting, but bursting remains self-limiting. Voltage and raster plot representations as in previous figure.

Simulated bicuculline application (disinhibition) in the setting of MFS produced greater GC firing at all percentages assessed (Fig. 6). Again, sustained oscillations were not seen even with very high levels of MFS.

We looked at a variety of stimulation paradigms in order to determine whether a different type of activation could produce a more sustained excitability in the network. Stimulation of a single GC simulates the effect of using an intracellular stimulating electrode. This provides far weaker stimulation than the PP activation used in the previous figures since the latter activated all of the GCs simultaneously. With inhibitory blockade, intermediate levels of MFS with this single-cell stimulation produced more sustained excitation than was seen with the stronger PP stimulation (Fig. 7). Without MFS or at extremely low levels of MFS, recurrent excitation was insufficient to produce any spread of activity, resulting in firing only in the one stimulated neuron (0%, arrow). With slightly more MFS varying patterns of sustained GC spiking were seen (1%). With still greater MFS, however, a pattern of stereotyped population response increasingly emerged. The seeming paradox of increasingly powerful excitatory connections producing progressively less sustained firing is readily explained by noting that with increasing synaptic drive onto other GCs, the single stimulated GC had a global effect on all GCs similar to that produced by PP stimulation. Therefore, all the GCs would fire together in a pattern similar to that seen in Fig. 5.

4. Discussion:

We have modeled the dentate gyrus, an area of the hippocampus that is believed to play an important role in the genesis of temporal lobe epilepsy. This relatively simple circuit demonstrates some surprising features both due to the richness of its recurrent connectivity and due to the unusual intrinsic properties of the neurons in this area. In particular, the principal neuron, the GC, has a high threshold for firing due to a resting membrane potential far from threshold, and has strong adaptation that prevents it from firing multiple times when this threshold is reached. Even in the setting of disinhibition or recurrent excitatory connections due to MFS, firing in these cells was still quite restricted. Interestingly, under certain conditions, relatively weak stimulation was able to produce sustained firing where stronger stimulation did not.

4.1. Value of realistic neuronal network modeling in modeling epilepsy

The use in this study of compartmental models of neurons incorporating time-dependent voltage-sensitive currents presents some clear disadvantages relative to the more familiar McCulloch-Pitts style units commonly used in artificial neural network (ANN) modeling. First there is the disadvantage of time since these networks run several orders of magnitude slower than ANNs of comparable size. Second, the effort to make the models relatively realistic constantly runs into the

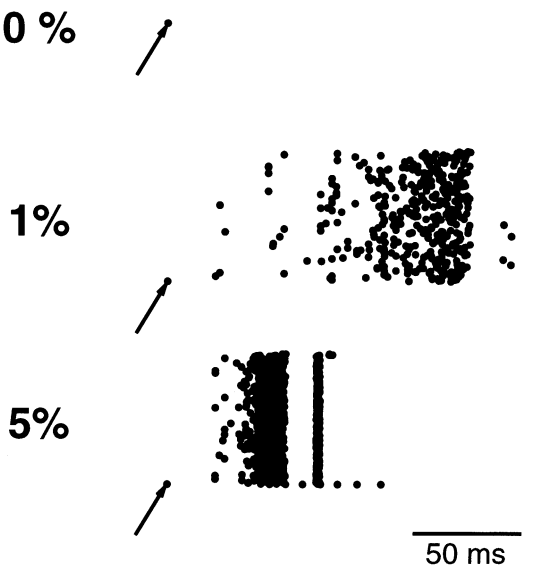

Fig. 7. Firing of GCs in $GABA_A$ disinhibited network (bicuculline simulation) with 0, 1 and 5% MFS in response to single neuron stimulation. With no MFS (0%) a single spike is seen in the stimulated cell with no spread to any other cells. With 1% MFS, relatively prolonged network activity is seen. With 5% MFS, a brief, fairly synchronous, response occurs.

limitations of unknown or sometimes unknowable parameters (but see below). Third, the complexity of these networks introduces substantial difficulties of analysis and interpretation. Despite these problems, we believe that it is important to utilize this type of network in epilepsy modeling in order to make direct connections with physiological experiments and, eventually, with the clinical disease of epilepsy.

Several findings in the current study demonstrate nonlinear interactions or time-dependent phenomenon that could not be readily reproduced with ANN units. Our discussion of shunting inhibition demonstrates how input that appears excitatory may have inhibitory effects. In fact, there is physiological evidence that these inputs may in some cases be excitatory, producing action potentials in GCs [46]. Another highly nonlinear phenomenon illustrated here is the phenomenon of depolarization block which can cause a heavily stimulated neuron to produce very little output (MC in Fig. 4). Although one could, of course, alter the nonlinear state function of an ANN unit to account for this drop-off, it is unlikely that simple analysis of the single cell physiology would have suggested such a major change in the standard ANN model.

Having built this relatively realistic neuronal network, it would now be possible to base an ANN on this model, as has been done in other areas of hippocampus [27]. This would provide a more tractable model that might allow further analytic insight into the interactions we illustrated here. Subsequently, however, it will be necessary to return to the more realistic model in order to make predictions that can be used in animal models to suggest surgical or pharmacological interventions, in order that such interventions may eventually be introduced in the treatment of human epilepsy.

4.2. Adaptation as intrinsic inhibition

The unusual properties of GCs give them a distinctive firing pattern that in turn determines the behavior of the network as a whole. GCs have a very low resting membrane potential. This means that they start out very far from spike threshold. Furthermore, they appear to have relatively high concentrations of voltage and calcium sensitive potassium channels that repolarize the cell after a spike and may then maintain the cell in a prolonged relative refractory period. Taken together, these influences make it hard to get a GC to fire once and very hard to get it to fire more than once. Hence, only one spike is seen even with the complete removal of inhibitory influences (Fig. 4).

Since the GC is the major input location, receiving afferents from entorhinal cortex, and is also the output cell of the dentate gyrus, the major role of intrinsic cellular factors on granule cell firing governs the network as well. In particular, network output tends to be fairly stereotyped as each granule cell follows its own tendencies rather than being strongly reactive to other firing in the network. Interestingly, this dominance of intrinsic GC dynamics was also seen in the simulations with MFS, despite the fact that in this case the granule cells were interconnected and could influence each others' firing. Though each GC was

activated similarly and responded similarly, they generally received very similar inputs from the other GCs, maintaining the stereotypy of firing. The only way that we were able to avoid GC stereotypy was to provide an extremely weak input (single cell stimulation) with relatively weak MFS connectivity. This tended to produce GC activations near activation threshold, allowing more variability in exact spike timing and in the pattern of recruitment of other cells. We would predict from this that another way of obtaining prolonged recruitment network activity of this sort would be to use very weak connections with high density MFS connectivity. However, this is unlikely to be a realistic pathological scenario.

The brief, heavily synchronized behavior we produced with PP input and the prolonged smoldering activity seen with the single cell stimulation would be expected to have very different effects on CA3 and on other networks downstream in the circuit. We would predict that these responses would tend to mimic the dentate gyrus pattern with high amplitude activity giving rise to brief hypersynchrony and prolonged activity begetting prolonged activity. The ability of this smoldering activity to provide continuing pathological activation suggests that this pattern might in fact be more detrimental than high-amplitude self-limiting hypersynchrony. These considerations suggest a further counterintuitive hypothesis: the brief hypersynchrony of the interictal spike or even of a brief seizure may actually serve a protective role as it quickly involves all the cellular elements and exhausts the potential for further interruption of normal neuronal processing.

4.3. Bootstrapping the connectivity matrix

As mentioned above, uncertainty about parameter values is a constant concern when trying to make models as realistic as practicable. In the current study, our ability to utilize parameters obtained from current clamp and dual impalement study gave us some confidence in the validity of both the intrinsic cellular parameters and most of the synaptic parameters. However, a critical set of parameters that cannot yet be adequately determined using current experimental techniques is the detailed connectivity matrix or wiring diagram of the network [2,25].

The most obvious way to determine connectivity in a brain area is to simply look, using anatomical methods. However, the existence of an anatomically defined synapse does not guarantee that it is physiologically functional. Furthermore, the practical limitations of light and electron microscopy make any such attempt daunting: precise synaptic identification can only be confirmed under electron microscopy while cell identification is best done with light microscopy. It is now possible to obtain detailed axonal tracings of single cells in order to define terminal fields where connections are made [29–31]. However, such data fails to identify the type of cell the axons are synapsing onto and also gives no information regarding whether synapses are physiologically active. Furthermore, the tracing of a single cell is a laborious process, which makes it impractical to build up a large-enough data set to fully reconstruct the connectivity matrix of a brain area. As an alternative, physiological investigations have the advantage of telling whether a synaptic

connection is an active one and giving further information about its strength and type, whether excitatory or inhibitory [23]. The type of investigation required to directly assess connectivity, dual simultaneous intracellular recording, is also extremely technically difficult, hence impractical as a technique for building up a large data set.

Of course, many techniques can and are brought to bear in combination to determine connectivity. We propose computer modeling as yet another technique that can be used to help elucidate this highly elusive aspect of neural organization. Although the lack of connectivity information makes precise modeling difficult, the power of computer models to explore vast numbers of possibilities makes it possible to assay many different connectivity percentages to determine ones that yield physiologically realistic results. By itself, this is a standard modeling technique that was utilized in parts of the present study to determine plausible parameter ranges. Coupled with physiological investigation, however, the same technique holds promise as a way to guide investigation by making progressively more detailed predictions about complex experimental paradigms that would otherwise be impossible to interpret. The situation would be analogous to a genetic algorithm with the physiological experiment providing the fitness function, since the physiological results can be used to select parameter ranges for further exploration. Selected parameter sets within these ranges can then be used to make more detailed predictions in a continuing bootstrap procedure.

In the current study, we used this technique to provide an estimate for the likely density of functional MFS in the kindling model by correlating our models with physiological study of both the inhibited and disinhibited slice. We predict from this that functional GC → GC MFS in kindled animals probably lies between 1 and 5%. Our findings further lead us to predict that such seemingly minor sprouting could have important effects.

5. Conclusion

Understanding epilepsy will require making conceptual connections between the molecular realm where anticonvulsant drugs work, the neuronal realm where most experimental studies are performed and the network realm where the disorder is manifest. Computer modeling provides the means to connect these levels. It is a method particularly well suited to dynamical diseases such as epilepsy where the concept of direct cause and effect may have to give way to the difficulties of tracking emergent phenomena in complex systems.

In this study we have looked at the development of various firing patterns in the dentate gyrus and found it to be remarkably resistant to perturbation. Only combining disinhibition with the new excitatory connections of MFS made a large difference in activity patterns. Even with these changes, ongoing self-regenerative activity was only seen under particular circumstances. Connecting the dentate gyrus model to a model of CA3, the next area in the hippocampal trisynaptic pathway, may give further insights into epileptogenesis and seizure propagation.

Acknowledgements

This research was supported by the Office of Research and Development, Medical Research Service of the Department of Veterans Affairs (WWL, KMH) by the National Institute of Neurological Disease and Stroke (WWL, TPS), by the Epilepsy Foundation of America (KMH) and by the Klingenstein Foundation (TJS).

References

[1] Amaral D. A Golgi study of cell types in the hilar region of the hippocampus in the rat. J Comp Neurol 1978;182:851–914.
[2] Amaral D, Ishizuka N, Claiborne B. Neurons, numbers and the hippocampal network. Progress in Brain Research. Amsterdam: Elsevier, 1990.
[3] Babb T, Kupfer W, Pretorius J, Crandall P, Levesque M. Synaptic reorganization by mossy fibers in human epileptic fascia dentate. Neuroscience 1991;42:341–63.
[4] Babb T, Pretorius J, Mello L, Mathern G, Levesque M. Synaptic reorganizations in epileptic human and rat kainate hippocampus may contribute to feedback and feedforward excitation. Epilepsy Res 1992;36:193–203.
[5] Bekenstein J, Rempe D, Lothman E. Decreased heterosynaptic and homosynaptic paired pulse inhibition in the rat hippocampus as a chronic sequela to limbic status epilepticus. Brain Res 1993;601:111–20.
[6] Buckmaster P, Schwartzkroin P. Interneurons and inhibition in the dentate gyrus in vivo. Neuroscience 1995;15:774–89.
[7] Cavazos J, Golarai G, Sutula T. Mossy fiber synaptic reorganization induced by kindling—time course of development, progression, and permanence. J Neurosci 1991;11:2795–803.
[8] Destexhe A, Contreras D, Sejnowski T, Steriade M. Modeling the control of reticular thalamic oscillations by neuromodulators. Neuroreport 1994a;5:2217–20.
[9] Destexhe A, Mainen Z, Sejnowski T. Synthesis of models for excitable membranes, synaptic transmission and neuromodulation using a common kinetic formalism. J Comput Neurosci 1994;1:195–230.
[10] Fricke R, Prince D. Electrophysiology of dentate gyrus granule cells. J Neurophysiol 1984;51:195–209.
[11] Golarai G, Sutula T. Bilateral organization of parallel and serial pathways in the dentate gyrus demonstrated by current-source density analysis in the rat. J Neurophysiol 1996;75:329–42.
[12] Golarai G, Sutula T. Functional alterations in the dentate gyrus demonstrated by current source density analysis after induction of long-term potentiation and kindling. J Neurophysiol 1996;75:343–53.
[13] Hines M. A program for simulation of nerve equations with branching geometries. Int J Biomed Comput 1989;24:55–68.
[14] Houser C, Miyashiro J, Swartz B, Walsh G, Rich J. Altered patterns of dynorphin immunoreactivity suggest mossy fiber reorganization in human hippocampal epilepsy. J Neurosci 1990;10:267–82.
[15] Isokawa M, Levesque M, Babb T, Engel J. Single mossy fiber axonal systems of human dentate granule cells studied in hippocampal slices from patients with temporal lobe epilepsy. Neuroscience 1993;13:1511–22.
[16] Lanerolle N, Kim J, Robbins R, Spencer D. Hippocampal interneuron loss and plasticity in human temporal lobe epilepsy. Brain Res 1989;495:387–95.
[17] Lytton W. Brain organization: from molecules to parallel processing. In: Trimble M, Cummings J, editors. Contemporary Behavioral Neurology, Ch. 1. Newton, MA: Butterworth–Heinemann, 1997:5–28.

[18] Lytton W. Adapting a feedforward heteroassociative network to Hodgkin-Huxley dynamics J Comput Neurosci (in press).
[19] Lytton W, Contreras D, Destexhe A, Steriade M. Dynamic interactions determine partial thalamic quiescence in a computer network model of spike-and-wave seizures. J Neurophysiol 1997;77:1679–96.
[20] Mathern G, Babb T, Mischel P, Vinters H, Pretorius J, Leite J. Childhood generalized and mesial temporal epilepsies demonstrate different amounts and patterns of hippocampal neuron loss and mossy fibre synaptic reorganization. Brain 1996;119:965–87.
[21] Merzenich M, Kaas J. Reorganization of mammalian somatosensory cortex following peripheral nerve injury. Trend Neurosci 1982;5:434–6.
[22] Merzenich M, Sameshima K. Cortical plasticity and memory. Curr Opin Neurobiol 1993;3:187–96.
[23] Miles R, Wong R. Unitary inhibitory synaptic potentials in the guinea-pig hippocampus in vitro. J Physiol (Lond) 1984;356:97–113.
[24] Nudo R, Milliken G. Reorganization of movement representations in primary motor cortex following focal ischemic infarcts in adult squirrel monkeys. J Neurophysiol 1996;75:2144–9.
[25] Patton P, McNaughton B. Connection matrix of the hippocampal formation. Hippocampus 1995;5:245–86.
[26] Pinsky P, Rinzel J. Intrinsic and network rhythomogenesis in a reduced Traub model for CA3 neurons. Comput Neurosci 1994;1:39–60.
[27] Pytte E, Grinstein G, Traub R. Cellular automaton models of the CA3 region of the hippocampus. Network 1991;2:149–67.
[28] Represa A, Salle G, Ben-Ari Y. Hippocampal plasticity in the kindling model of epilepsy in rats. Neurosci Lett 1989;99:345–50.
[29] Rockland K. Configuration, in serial reconstruction, of individual axons projecting from area V2 to V4 in the macaque monkey. Cereb Cortex 1992a;2:353–74.
[30] Rockland K. Laminar distribution of neurons projecting from area V1 to V2 in macaque and squirrel monkeys. Cereb Cortex 1992b;2:38–47.
[31] Rockland K, Saleem K, Tanaka K. Divergent feedback connections from areas V4 and TEO in the macaque. Visual Neurosci 1994;11:579–600.
[32] Scharfman H. Blockade of excitation reveals inhibition of dentate spiny hilar neurons recorded in rat hippocampal slices. J Neurophysiol 1992;68:978–84.
[33] Scharfman H. Differentiation of rat dentate neurons by morphology and electrophysiology in hippocampal slices: granule cells, aspiny cells, and spiny hilar neurons. Epilepsy Res 1992;S7:93–109.
[34] Scharfman H, Kunkel D, Schwartzkroin P. Synaptic connections of dentate granule cells and hilar neurons: Results of paired intracellular recordings and intracellular horseradish peroxidase injections. Neuroscience 1990;37:693–707.
[35] Scharfman H, Schwartzkroin P. Protection of dentate hilar cells from prolonged stimulation by intracellular calcium chelation. Science 1989;246:257–60.
[36] Sloviter R. Possible functional consequences of synaptic reorganization in the dentate gyrus of kainate-treated rats. Neurosci Lett 1992;137:91–6.
[37] Staley K, Otis T, Mody I. Membrane properties of dentate gyrus granule cells—comparison of sharp microelectrode and whole-cell recordings. J Neurophysiol 1992a;67:1346–58.
[38] Sutula T, Cascino G, Cavazos J, Parada I, Ramirez L. Mossy fiber synaptic reorganization in the epileptic human temporal lobe. Ann Neurol 1989;26:321–30.
[39] Sutula T, He X, Cavazos J, Scott G. Synaptic reorganization in the hippocampus induced by abnormal functional activity. Science 1988;239:1147–50.
[40] Sutula T, Zhang P, Lynch M, Sayin U, Golarai G, Rod R. The spatial distribution and morphological characteristics of sprouted mossy fiber axons in the dentate gyrus of kainate-treated rats. J Comput Neurol 1998;390:578–94.
[41] Traub R, Knowles W, Miles R, Wong R. Synchronized after discharges in the hippocampus: simulation studies of the cellular mechanism. Neuroscience 1984;12:1191–200.
[42] Traub R, Miles R. Neuronal Networks of the Hippocampus. New York: Cambridge University Press, 1991.

[43] Traub R, Miles R, Wong R. Models of synchronized hippocampal bursts in the presence of inhibition I single population events. J Neurophysiol 1987;58:739–51.
[44] Traub R, Miles R, Wong R, Schulman L, Schneiderman J. Models of synchronized hippocampal bursts in the presence of inhibition. II. Ongoing spontaneous population events. J Neurophysiol 1987;58:752–64.
[45] Traub R, Wong R. Cellular mechanisms of neuronal synchronization in epilepsy. Science 1982;216:745–7.
[46] Williamson A, Telfeian A, Spencer D. Prolonged GABA responses in dentate granule cells in slices isolated from patients with temporal lobe sclerosis. J Neurophysiol 1995;74:378–87.
[47] Wuarin J, Dudek F. Electrographic seizures and new recurrent excitatory circuits in the dentate gyrus of hippocampal slices from kainate-treated epileptic rats. J Neurosci 1996;16:4438–48.